JOURNAL OF OPTOELECTRONICS AND ADVANCED MATERIALS, Vol. 11, No. 6, June 2009, p. 857 - 862

Aloe vera solution synthesis and magnetic properties of Ni-Cu-Zn ferrite nanopowders

P. LAOKUL[a], S. MAENSIRI[a,b*]
[a]*Small & Strong Materials Group, Department of Physics, Faculty of Science, Khon Kaen University, Khon Kaen, 40002, Thailand*
[b]*Integrated Nanotechnology Research Center (INRC), Faculty of Science, Khon Kaen University, Khon Kaen, 40002, Thailand*

$Ni_xCu_{0.25}Zn_{0.75-x}Fe_2O_4$ (x = 0.25, 0.35, 0.5) nanopowders were prepared by a simple solution method using metal nitrates and aloe vera plant extracted solution. The prepared samples were characterized by XRD, FT-IR, SEM, TEM and VSM. All the prepared samples are polycrystalline and have spinel structure with the particle sizes of ~15-40 nm. The samples exhibit ferromagnetic behavior, having saturation magnetization and coercivity values in the range of 32.52–66.58 emu/g at 10 kOe and 58.46-140.47 Oe, respectively.

(Received November 4, 2008; accepted June 15, 2009)

Keywords: Ni-Cu-Zn ferrite; Nanopowders; Magnetic properties; Synthesis; Electron microscopy

1. Introduction

Ni-Cu-Zn ferrites are soft magnetic materials that are used for inductive multilayer devices because of the materials relatively low sintering temperature and their good magnetic and dielectric properties at intermediate to high frequency. The sintering temperature of the ferrite is limited to less than 950 ^oC, which is the melting point of Ag used as internal conductor in the multilayer devices [1]. Various methods have been developed to synthesize nanocrystalline Ni-Cu-Zn ferrites, including citrate precursor techniques [2], coprecipitation [3-6], sol–gel [7-9], and conventional ceramic techniques [10-15]. Among these established synthesis methods, it is still critical to find simple and cost effective routes to synthesize nanocrystalline Ni-Cu-Zn ferrites by utilization of cheap, nontoxic and environmentally benign precursors.

Recently, biosynthetic methods employing either biological microorganisms or plant extracts have emerged as a simple and viable alternative to chemical synthetic procedures and physical methods. There are many reports on the syntheses of metal and semiconductor nanoparticles using fungi, actinomycetes and plant extracts. Chandral et. al. have demonstrated synthesis of gold nanotriangles and silver nanoparticles using aloe vera plant extracts as a reducing agent. In their work, the sizes of nanotriangle gold are about 50-350 nm and spherical nanosilvers are about 5-15 nm [16].

Aloe vera is a native plant in Thailand and several other countries. There is 98.5% water content in the aloe vera leaves. The rest are some ingredients including polysaccharides (pectins, hemicelluloses, glucomannan, acemannan, and mannose derivatives). It also contains amino acids, lipids, sterols (lupeol, campesterol, and β-sitosterol0, tannins, and various enzymes. Aloe vera gel is widely used in the cosmetics industry as a hydrating ingredient in liquids, creams, sun lotions, lip balms, healing ointments etc. The gel is further used in pharmacology for wound healing, anti inflammatory and burn treatment [17]. Most recently our group has reported the use of aloe vera plant for the synthesis of indium oxide nanoparticles with particle size of 5-50 nm [18].

In this work we investigated a series of Ni-Cu-Zn ferrite nanopowders with variation of copper content by a modified aloe vera solution route. Using of aloe vera extract simplifies the process and provides an economical alternative process for synthesis of ferrite nanopowders. We found that $Ni_xCu_{0.25}Zn_{0.75-x}Fe_2O_4$ (x = 0.25, 0.35, 0.5) offered the optimum magnetic properties, which we report in detail below.

2. Experimental

In this study, $Ni(NO_3)_2.6H_2O$ (>99% purity, BDH Laboratory Supplies), $Cu(NO_3)_3.3H_2O$ (99.5% purity, Carlo Erba Reacgenti), $Zn(NO_3)_2.6H_2O$ (99% purity, Fluka), $Fe(NO_3)_3.9H_2O$ (>99% purity, BDH Laboratory Supplies) and aloe vera extract were used as the starting materials. In a typical procedure, 250 ml aloe vera extract was first stirred at room temperature until a homogeneous solution was obtained. According to the formula $Ni_xCu_{0.25}Zn_{0.75-x}Fe_2O_4$ (x = 0.25, 0.35, 0.5), each metal nitrate was added slowly to the aloe vera solution under vigorous stirring for 2 h to obtain a well-dissolved solution. Then, the mixed solution was evaporated by heating on the hot plate at 150 ^oC under vigorous stirring for several hours until a dried precursor was obtained. The dried precursor was crushed into powder using mortar and pestle. In order to determine the temperature of possible decomposition and crystallization of the nanopowders, the dried precursor was subjected to thermogravimetric-differential thermal analysis (TG-DTA) (Pyris Diamond TG-DTA, Perkin Elmer Instrument). The dried precursor then was calcined in a box-furnace and characterized by powder X-ray Diffraction (XRD) using X-ray diffractometer (PW3040, Phillips, The Netherlands) with CuK_α radiation (λ = 0.15406 nm). Fourier transform infrared (FT-IR) spectra of the powders (as pellets in KBr) were recorded using a Fourier transform infrared spectrometer (Spectrum One FT-IR Spectrometer, Perkin

Elmer Instrument, USA) in the range of 4000-370 cm^{-1}. The particle size and morphology of the calcined powders were characterized by scanning electron microscopy (LEO SEM 1450VP, UK) and transmission electron microscopy (TEM, JEOL 2010, 200kV, Japan). The magnetic properties of the precursors and the calcined powders were examined at room temperature (20 ^{o}C) using a vibrating sample magnetometer (VSM 7403, Lake Shore, USA).

3. Results and discussion

The obtained precursors were characterized by TG/DTA (Fig. 1) to determine the thermal decomposition. The DTA-curve showed endothermic peaks around 90, 210, and 280 ^{o}C, which are correlated to the sharp weight losses due to the removal of water and nitrate on the TG-curve [19]. The final step of thermal degradation around 540 ^{o}C might be correlated to the complete decomposition of pure salt to metal oxide.

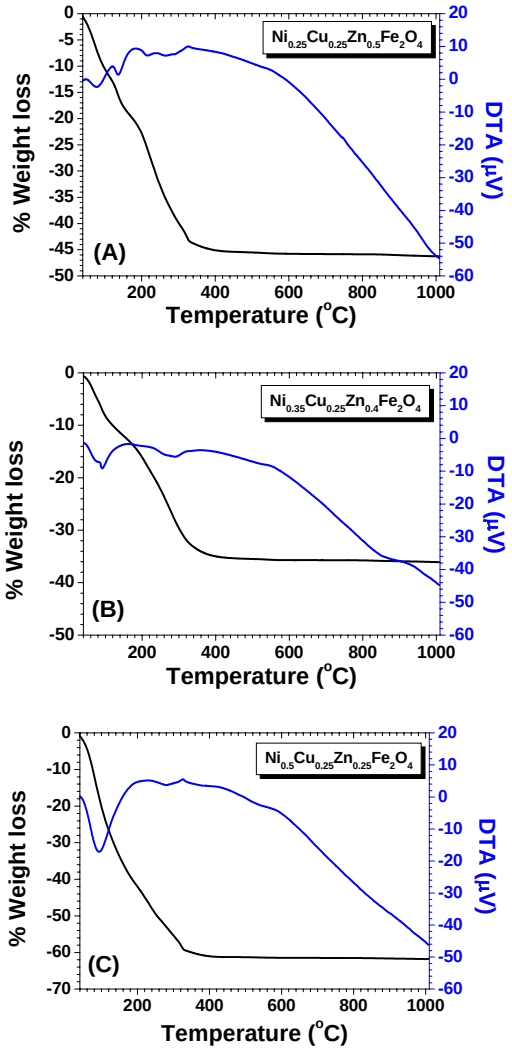

Fig. 1. TG/DTA curves of Ni-Cu-Zn precursors using heating rate of 10°C/min from 40 to 1000°C. (A) $Ni_{0.25}Cu_{0.25}Zn_{0.5}Fe_2O_4$, (B) $Ni_{0.35}Cu_{0.25}Zn_{0.4}Fe_2O_4$, and (C) $Ni_{0.5}Cu_{0.25}Zn_{0.25}Fe_2O_4$.

Note that there was no more weight loss after 550 ^{o}C suggesting that the solid-solid interaction between the produced oxides to form Ni-Cu-Zn ferrites crystalline can be found at T > 550 ^{o}C. To obtain crystalline nanoparticles, the prepared precursor was calcined in air for 2 h at 500, 600, 700, 800 and 900 ^{o}C. The formation of nanocrystalline Ni-Cu-Zn ferrites was confirmed by XRD and FT-IR analysis, shown in Figure 2 and 3, respectively.

The XRD results (Fig. 2) confirmed the formation of cubic structure ferrite, which exactly matches the JCPDS card No. 87-2334. No diffraction peaks of other impurities such as α-Fe_2O_3 or CuO were observed. From X-ray line broadening of the reflection of (311) which is the highest intensity peak in XRD patterns, the average crystalline sizes (D) of sample were determined by the Scherrer equation ($D = 0.89\lambda/(\beta\cos\theta)$, where λ is the wavelength of the X-ray radiation, θ is the diffraction angle and β is the full width at half maximum (FWHM) [20]). As shown in Table 1, the higher the calcination temperature, the bigger the particle size. However, the chemical compositions and calcination temperature do not significantly change the lattice parameter of Ni-Cu-Zn ferrites. The values of the lattice parameter a are close to 0.8398 nm that reported for Fe_3O_4 in the standard report data (JCPDS: 87-2334).

Table 1. Average particle sizes and lattice parameter a calculated from XRD spectra, the specific magnetization (M_s) and coercive forces (H_c) of the Ni-Cu-Zn samples calcined in air for 2 h at 600, 700, 800 and 900 °C.

Materials	Calcination temperature	Particle size (nm) from XRD	Lattice parameter a (nm)	M_s (emu/g) at 10 kOe	H_c (Oe)
$Ni_{0.25}Cu_{0.25}Zn_{0.5}Fe_2O_4$	600 °C	15.9	0.83810 ± 0.00011	39.50	63.06
	700 °C	21.6	0.83945 ± 0.00005	47.76	92.39
	800 °C	28.8	0.83809 ± 0.00015	53.58	98.17
	900 °C	40.7	0.83905 ± 0.00006	58.11	61.00
$Ni_{0.35}Cu_{0.25}Zn_{0.4}Fe_2O_4$	600 °C	15.7	0.83601 ± 0.00036	39.83	58.46
	700 °C	20.7	0.83824 ± 0.00013	50.47	98.68
	800 °C	28.9	0.83917 ± 1.3E-06	60.70	108.15
	900 °C	40.1	0.83938 ± 0.00005	66.58	66.54
$Ni_{0.5}Cu_{0.25}Zn_{0.25}Fe_2O_4$	600 °C	14.7	0.83756 ± 0.00004	32.52	97.30
	700 °C	19.6	0.83700 ± 0.00001	42.60	138.79
	800 °C	21.4	0.83801 ± 0.00004	51.31	140.47
	900 °C	37.2	0.83688 ± 0.00009	59.43	92.46

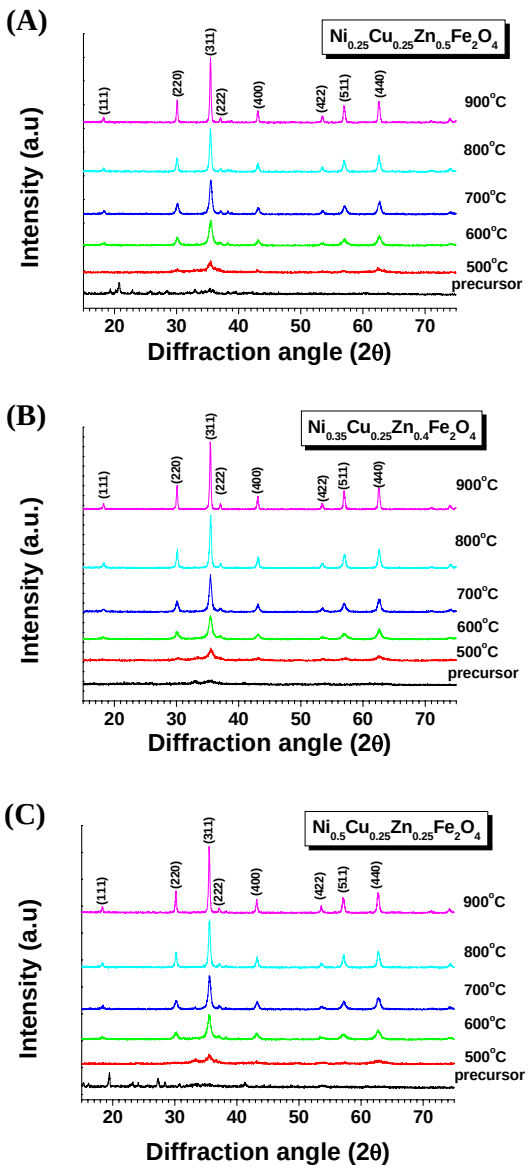

Fig. 2. XRD patterns of Ni-Cu-Zn precursors and Ni-Cu-Zn samples calcined in air for 2 h at 500, 600, 700, 800 and 900 °C. (A) $Ni_{0.25}Cu_{0.25}Zn_{0.5}Fe_2O_4$, (B) $Ni_{0.35}Cu_{0.25}Zn_{0.4}Fe_2O_4$, and (C) $Ni_{0.5}Cu_{0.25}Zn_{0.25}Fe_2O_4$.

In order to confirm the formation of the spinel phase and to understand the nature of the residual carbon in the samples, the FTIR spectra of the as-synthesized powders and thermally treated powders were recorded. The results from FTIR technique are presented in Fig. 3. The calcined samples show characteristic absorptions of ferrite phase with a strong absorption around 600 cm^{-1} and weak absorption in the range 399-427 cm^{-1}. This difference in the spectral positions is expected because of the difference in the M^{+}-O^{2}- distance for the octahedral and tetrahedral compounds. Waldron [21] studied the vibrational spectra of ferrites and attributed the sharp absorption band around 600 cm^{-1} to the intrinsic vibrations of the tetrahedral groups and the other bands the octahedral groups. There are two weak and broad absorption peaks at around 1400 and 1600 cm^{-1} corresponding to the presence of small amounts of residual carbon in the samples. These absorptions in the present case are very weak which indicates that the residual carbon has mostly burnt away during the calcination process.

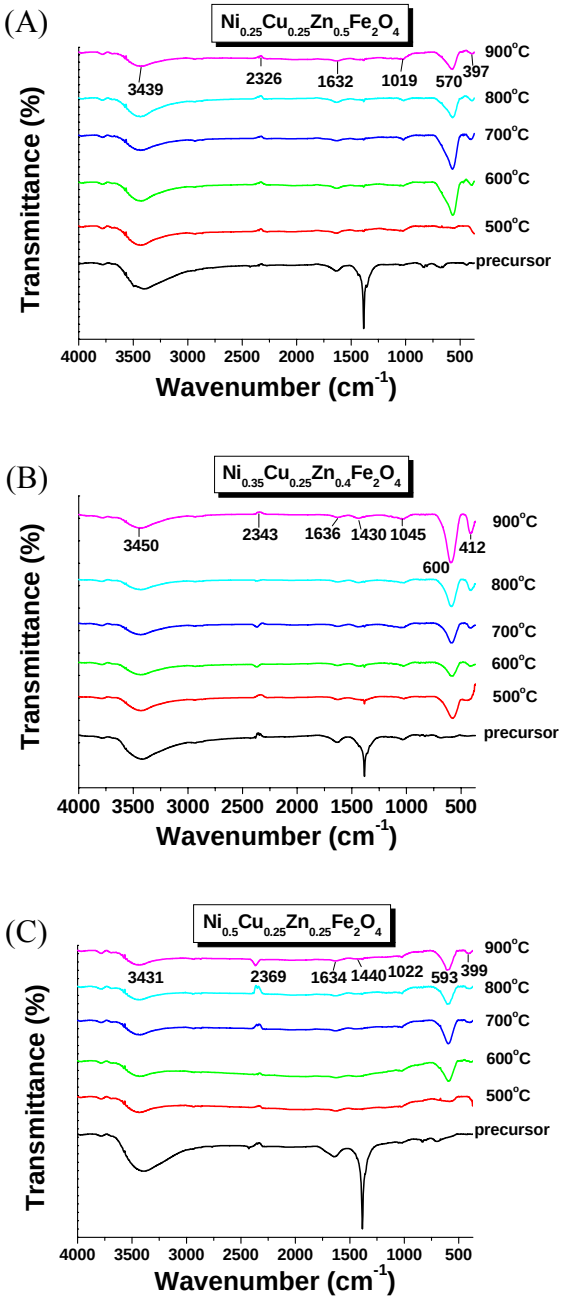

Fig. 3. FT-IR spectra of Ni-Cu-Zn precursors and Ni-Cu-Zn samples calcined in air for 2 h at 500, 600, 700, 800 and 900 °C. (A) $Ni_{0.25}Cu_{0.25}Zn_{0.5}Fe_2O_4$, (B) $Ni_{0.35}Cu_{0.25}Zn_{0.4}Fe_2O_4$, and (C) $Ni_{0.5}Cu_{0.25}Zn_{0.25}Fe_2O_4$.

The morphology of the prepared ferrite powders was revealed by SEM and TEM techniques (Fig. 4). The sample calcined at 700 ^{o}C consists of < 100 nm clusters of particles. It shows that the chemical composition affects morphologies of the samples: some are spheres, some are rods. Figure 4 shows bright-field TEM images of the 700 ^{o}C calcined particles of around 15-30 nm diameter. The corresponding selected-area electron diffraction (SAED) patterns of all the samples show spotty ring patterns of cubic structure ferrite. The measured interplanar spacings (d_{hkl}) from selected-area electron diffraction patterns in Fig. 4 are in good agreement with the XRD data and the value in standard data (JCPDS: 87-2334).

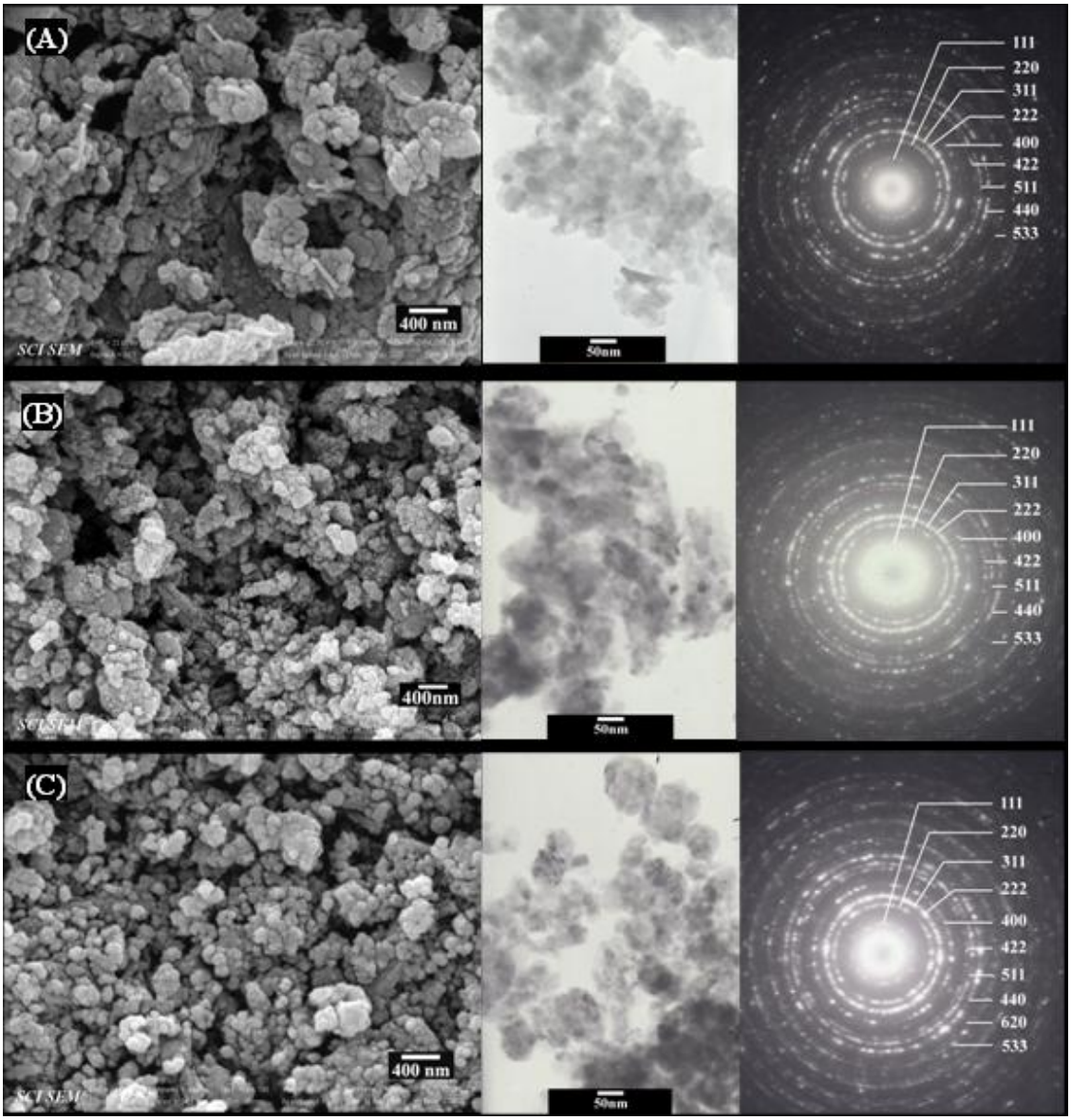

Fig. 4. SEM micrographs (left) and TEM images with corresponding selected area diffraction patterns (right) of the Ni-Cu-Zn samples calcined in air at 700 ^{o}C for 2 h. (A) $Ni_{0.25}Cu_{0.25}Zn_{0.5}Fe_2O_4$, (B) $Ni_{0.35}Cu_{0.25}Zn_{0.4}Fe_2O_4$, and (C) $Ni_{0.5}Cu_{0.25}Zn_{0.25}Fe_2O_4$.

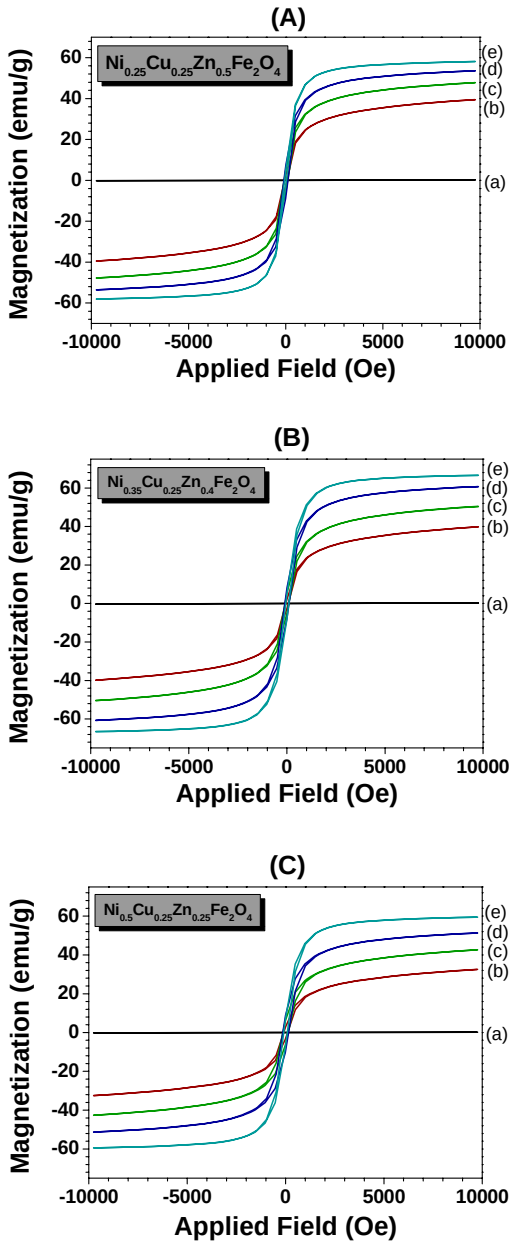

Fig. 5. The specific magnetization of (a) Ni-Cu-Zn precursors and Ni-Cu-Zn samples calcined in air for 2 h at temperatures of (b) 600 °C, (c) 700 °C, (d) 800 °C, and (e) 900 °C, as a function of field, measured at 20 °C. (A) $Ni_{0.25}Cu_{0.25}Zn_{0.5}Fe_2O_4$, (B) $Ni_{0.35}Cu_{0.25}Zn_{0.4}Fe_2O_4$, and (C) $Ni_{0.5}Cu_{0.25}Zn_{0.25}Fe_2O_4$.

Room temperature specific magnetization (Fig. 5) results showed a weak ferromagnetic behavior in the precursor sample whereas the calcined samples have stronger ferromagnetic behavior in the field ranging between ±4000 Oe. The saturation-specific magnetization (M_s) was increased with increasing calcination temperature. It is found that the tendency of M_s to increase with increasing of calcination temperature corresponds to the enhancement of crystallinity and crystalline size of ferrites. This phenomenon can be explained using an assumption of a nonmagnetic layer on the surface of the particle. The increased M_s is due to the decreasing ratio of nonmagnetic volume to the total volume of the particles [22]. Fig. 6 shows the effect of the chemical composition on the specific magnetization of calcined samples. Among the studied ferrites $Ni_{0.35}Cu_{0.25}Zn_{0.4}Fe_2O_4$ has the highest specific magnetization. Note that this composition contains middle level of Ni and Zn. This is because the different compositions result in different particle sizes of ferrite samples as shown in Table 1. The value of coercivity (H_c) of samples increased with increasing temperature up to 800 °C and then decreases when the calcination temperature is at 900 °C as shown in Fig. 7.

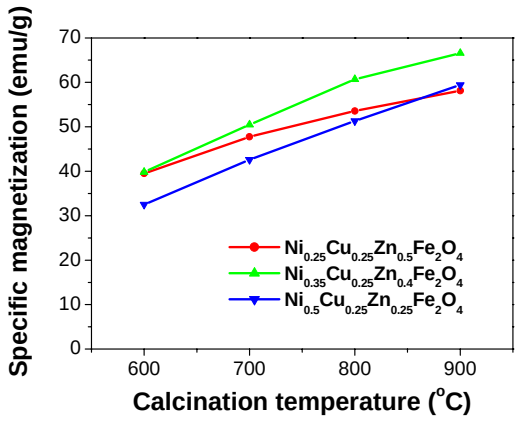

Fig. 6. Specific magnetization of ferrite samples calcined at difference temperatures.

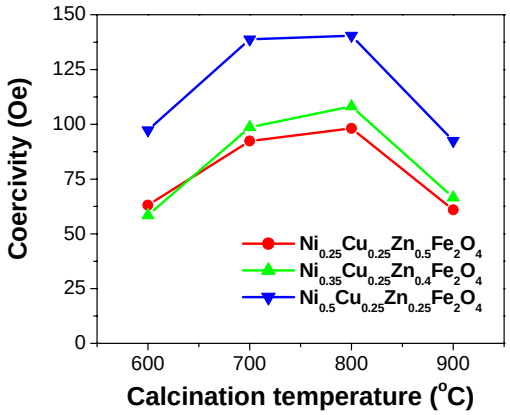

Fig. 7. Coercivity of ferrite samples calcined at difference temperatures.

This variation of H_c with calcination temperature can be explained on the basis of domain structure, critical size and anisotropy of crystals [23-25]. It is known that magnetization in ferrites proceeds through the movement of domain walls and domain rotations and the coercive force is obtained by reversal of the directions of the wall movement and that of domain rotation on reversing the direction of the applied magnetic field. In general, the energy associated with wall movement is less than that of domain rotation. The larger the particle size, the greater the probability of domain formation and domain rotation. On the other hand, the smaller particles contain less domain walls and require higher force for demagnetization [26]. For smaller particles of $Ni_{0.5}Cu_{0.25}Zn_{0.25}Fe_2O_4$, the probability of domain rotation is higher and consequently the coercive force obtained is higher. It is suggested from this work that the $Ni_{0.35}Cu_{0.25}Zn_{0.4}Fe_2O_4$ composition is the most useful ferrite because of its lowest coercivity (58-108 Oe**)** and highest magnetization (40-67 emu/g).

4. Conclusion

Using of metal nitrates and the aloe vera extract solution as starting materials, Ni-Cu-Zn ferrite nanopowders have been synthesized. From XRD, FT-IR spectra and electron diffraction analysis, it is indicated that the crystalline spinel ferrite can be obtained using calcination temperatures at 600-900 ^oC in air for 2h. The particle sizes of the nanocrystalline spinel ferrite calculated from the FWHM of the XRD (311) peak are in the range of 15-40 nm and in good agreement with TEM results. All of the samples are soft magnetic materials having strong specific magnetization from 32-67 emu/g with low coercivity of 58-140 Oe depending on their calcination temperatures and chemical compositions. Among investigated ferrites, the $Ni_{0.35}Cu_{0.25}Zn_{0.4}Fe_2O_4$ has highest specific magnetization of 67 emu/g and lowest coercivity of 58 Oe due to its large particle size. The present work proves that the Aloe vera plant-extracted solution synthesis is a new useful method using cheap precursors for preparation of Ni-Cu-Zn ferrite nanopowders. However, the role of the aloe vera extract is not yet specified. For example, complexation between aloe vera components and metal ions in the solution is still unknown, and this is under investigation.

Acknowledgments

The authors would like to thank Prof. Dr. Seraphins for their valuable suggestions during writing of this article, the Department of Chemistry, Khon Kaen University for providing TG-DTA, VSM and FTIR facilities, the Faculty of Science Electron Microscopy Unit, Khon Kaen University for providing SEM facilities. This work is supported by The Integrated Nanotechnology Research Center, Khon Kaen University, and The National Nanotechnology Center (NANOTEC), NSTDA, Ministry of Science and Technology, Thailand, through its program of Center of Excellence.

References

[1] K. O. Low, F.R. Sale, J. Magn. Magn. Mater. **256**, 221 (2003).
[2] X. H. Wang, W.G.Qu, L.T. Li, Ceram. Tran. **129**, 211 (2002).
[3] I. Z. Rahman, T. T. Ahmed, J. Magn. Magn. Mater. **290-291**, 1576 (2005).
[4] T. Krishnaveni, B. Rajini Kanth, V. Seetha Rama Raju, S.R. Murthy, J. Alloy. Comp. **414**, 282 (2006).
[5] M. Fujimoto, Y. Nishi, T. Suzuki, H. Shigetani, S. Sekiguchi, J. Am. Ceram. Soc. **81**, 2477 (1998).
[6] W.C. Hsu, S. C. Chen, P. C. Kuo, C. T. Lie, W. S. Tsai, Mater. Sci. Eng. B. **111**, 142 (2004).
[7] L. Yu, Shixun Cao, Yongshen Liu, Jiujing Wang, Chao Jing and Jincang Zhang, J. Magn. Magn. Mater. **31**, 100 (2006).
[8] S. Hahi, M. Hashim, A. R. Daud, Mater. Lett. **60**, 2803 (2006).
[9] W. C. Kim, S. I. Park, and S. J. Kim, J. Appl. Phys. **87**, 6241 (2000).
[10] T. Nakamura, J. Magn. Magn. Mater. **168**, 285 (1997).
[11] M. Fujimoto, J. Am. Ceram. Soc. **77**, 2873 (1994).
[12] J. Mürbe, J. Töpfer, J. Electroceram. **15**, 215 (2005).
[13] J. Mürbe, J. Töpfer, J. Electroceram. **16**, 199 (2006).
[14] O. F. Cultun, L. Spinu, A. Stancu, IEEE Trans. Magn. **37**, 2353 (2001).
[15] A. Pradeep, C. Thangasamy, G. Chandrasekaran, J. Mater. Sci. **15**, 797 (2004).
[16] S. P. Chandran, M. Chaudhary, R. Pasricha, A. Ahmad, Sastry M., Biotechnol. Prog. **22**, 577 (2006).
[17] Definition, Testing and Application of Aloe Vera and Aloe Vera Gel, www.nature4science.com, dowloaded in 12/06/2007.
[18] S. Maensiri, P. Laokul, J. Klinkaewnarong, S. Phokha, V. Promarak, S. Seraphin, Adv. Mater. Rapid Comm. **2**, 161 (2008).
[19] W. M. Shaheen, A. A. Ali. Int. J. Inorg. Mater. **3**, 1073 (2001).
[20] B. D. Cullity, S. R. Stock, Elements of X-ray Diffraction, 3nd ed.; Prentice Hall: New Jersey, 2001.
[21] R. D. Waldron, Phys. Rev. **99**, 1727 (1955).
[22] S. Yan, J. Geng, L. Yin, E. Zhou, J. Magn. Magn. Mater. **277**, 84 (2001).
[23] B.D. Cullity, Introduction to Magnetic Materials, Addison-Wesley Plublishing Co. Inc., Reading. MA.1972.
[24] S. Chikazumi, Physics of Magnetism, Wiley, New York, 1959.
[25] M. Georgea, A. Mary John, S. S. Naira, P.A. Joy, M. R. Anantharaman, J. Magn. Magn. Mater. **302**, 190 (2006).
[26] A. Verma, D. C. Dube, J. Am. Ceram. Soc., **88**, 519 (2005).

*Corresponding author: sanmae@kku.ac.th;
santimaensiri@gmail.com